Double ionization of helium by fast ion impact: Reexamination of the correlation function

L. Gulyás

Institute of Nuclear Research of the Hungarian Academy of Sciences (ATOMKI), P.O. Box 51, H-4001 Debrecen, Hungary

A. Igarashi

Department of Applied Physics, Faculty of Engineering, University of Miyazaki, 889-2192, Japan

T. Kirchner*

Institut für Theoretische Physik, TU Clausthal, Leibnizstraße 10, D-38678 Clausthal-Zellerfeld, Germany

The recently introduced correlation function [M. Schulz *et al.*, Phys. Rev. Lett. **84**, 863 (2000)] for the analysis of double ionization processes is reconsidered. We present a model based on the frozen-correlation and continuum distorted-wave with eikonal initial-state approximations, and compare numerical results with experimental data for double ionization in 100 MeV/amu C^{6+}-He and 3.6 MeV/amu Au^{53+}-He collisions. Our calculations confirm earlier conclusions about the primary and secondary roles of final-state and initial-state correlations, respectively. However, we show that the usual definition of the correlation function on the level of cross sections is problematic, since even a fully uncorrelated calculation gives rise to a nontrivial result. The intended limit of a zero-valued function for an independent electron calculation is achieved only if the analysis is performed on the level of impact-parameter dependent transition probabilities. Consequently, the workings of initial- and final-state correlations are reflected unambiguously only on this level.

PACS number(s): 34.10.+x, 34.50.Fa, 34.70.+e

I. INTRODUCTION

Double ionization (DI) of helium atoms or heliumlike ions by photon and charged-particle impact is one of the most simple and fundamental example of a correlated multiparticle transition. Accordingly, considerable experimental and theoretical efforts have been devoted to its detailed investigation and in-depth analysis [1,2]. In principle, a thorough understanding of this two-electron emission process requires consideration of the full kinematics, i.e., the determination of the momenta of all outgoing particles. This task continues to represent a great challenge for both experimentalists and theorists.

Kinematically complete experimental studies of electron-induced DI, the so-called $(e, 3e)$ process, date back to the beginning of the 1990s, and a wealth of seminal results have been accumulated and successfully explained since then (see Ref. [3] for a recent review). The experiments have been achieved in the high impact energy regime ($E_e \geq 500$ eV), where the interpretation can be based on first- or second-order perturbation theory. Moreover, in most cases kinematic situations have been studied, in which the scattering angle of the projectile is small and the momentum transferred to the target electrons amounts only to a small fraction of its initial momentum. Similar conditions are often realized in heavy-particle collisions [4], for which the *cold target recoil ion momentum spectroscopy* (COLTRIMS) technique provides a unique tool for studying multiple-ionization processes [5,6]. Using COLTRIMS the first (nearly) fully differential DI cross sections were recently reported for 6 MeV p-He collisions. They were compared with $(e, 3e)$ data obtained

for similar kinematic conditions to shed light on the projectile-charge sign dependence of the four-particle dynamics [7].

Obviously, fully differential cross sections contain the most detailed information about collisional processes. It is, however, not always clear whether and how specific signatures in the spectra can be related to specific causes, such as electron-correlation effects, postcollisional interactions, or the dynamics of the collision itself. In order to disentangle these effects and to elucidate particularly electronic correlations it was recently suggested to apply the concepts of intensity interferometry to doubly ionizing collisions [8]. A correlation function was defined as the ratio of the measured intensity for two-electron emission in a given event and the corresponding intensity for electrons from two independent events, and was sampled as a function of the momentum difference of both electrons for three different collision systems: 100 MeV/amu C^{6+}-He, 3.6 MeV/amu Au^{53+}-He, and 3.6 MeV/amu Au^{53+}-Ne. Remarkably, the data exhibited a very similar behavior in all three cases. It was concluded that the kinematics and dynamics effectively cancel out in this representation, and only "universal" characteristics of electronic correlations survive. Further analysis suggested that the final-state repulsion of the two outgoing electrons leaves its footprints rather directly in the correlation function and might conceal possible traces of initial-state correlations [8,9].

Calculations within the Born approximation and the shake-off model for DI supported the dominance of the final-state interaction for the 100 MeV/amu C^{6+}-He system [10]. Subsequent works were concerned with the correlation function for ionization from excited states [11], and with imposing certain kinematic conditions which rendered possible the observation of a strong initial-state dependence [12]. Very recently, it was argued that a differential version

---

*Electronic address: tom.kirchner@tu-clausthal.de

of the correlation function depending on the polar emission angles revealed the operation of a dipole selection rule, which could not be seen in the fully differential cross sections [13].

One may summarize these developments in the following way: (i) the correlation function appears to be a promising tool for extracting rather universal symmetry and electron-electron interaction effects from otherwise complicated collisions; (ii) theoretical support for this idea is so far limited to relatively simple first-order calculations. Accordingly, further theoretical analysis and calculations on the basis of a higher-order approximation seem appropriate and are the subject of this paper.

Based on the frozen-correlation [14] and the continuum distorted-wave with eikonal initial-state approximations [15,16] we have developed a model for the investigation of correlation effects in DI of helium. Our present numerical results for the correlation function do indeed confirm some of the reported trends, but our analysis leads also to an important caveat: the usual definition of the correlation function on the basis of cross sections is not completely satisfactory, since even a fully uncorrelated calculation gives rise to a nontrivial result. This contradicts the idea that structures in the correlation function can be unambiguously related to electron-correlation effects, and must therefore be kept in mind when conclusions are to be drawn.

We summarize the salient points of our theoretical model in Sec. II, present a detailed discussion of our results for the correlation function in Sec. III, and draw some conclusions in Sec. IV. A more detailed account of our model will be presented together with (multidifferential) cross section results in a forthcoming paper. Atomic units ($\hbar = m_e = e = 1$) are used throughout.

II. THEORY

As mentioned above our present calculations are based on the frozen-correlation approximation (FCA) of the two-electron dynamics within the impact parameter picture of the collisional interaction [14]. The basic idea of the FCA is to separate electronic correlations in the asymptotic initial and final states from those which might operate during the collision. It was argued that the latter can be neglected when the collision time is short compared to a suitably defined correlation time of the system [14]. This condition is met for the energetic collision systems 100 MeV/amu C^{6+}-He and 3.6 MeV/amu Au^{53+}-He that we consider in this work, i.e., we can restrict the incorporation of correlation effects to the initial and final states.

Accordingly, we assume the ground state of the He atom to be of the configuration interaction (CI) form

$$\Phi_o(\mathbf{x}_1, \mathbf{x}_2) = \sum_{j_1 j_2} C_{j_1 j_2} \phi^{j_1}(\mathbf{x}_1) \phi^{j_2}(\mathbf{x}_2), \qquad (1)$$

and use the (approximate) ansatz

$$\Phi_{\mathbf{k}_1 \mathbf{k}_2}(\mathbf{x}_1, \mathbf{x}_2) = \frac{1}{\sqrt{2}} [(\phi_{\mathbf{k}_1}(\mathbf{x}_1) \phi_{\mathbf{k}_2}(\mathbf{x}_2) + \phi_{\mathbf{k}_1}(\mathbf{x}_2) \phi_{\mathbf{k}_2}(\mathbf{x}_1)] \varphi(k_{12})$$

$$(2)$$

for the two-electron continuum states. $\mathbf{x}_1$, $\mathbf{x}_2$, $\mathbf{k}_1$, and $\mathbf{k}_2$ denote the positions and momenta of the electrons, respectively, and $k_{12} = |\mathbf{k}_1 - \mathbf{k}_2|$ is their momentum difference. In the case of Eq. (1) we use the ground-state wave function of Ref. [17] that includes both radial and angular correlations and yields 80% of the total correlation energy of the He atom. According to this model, the $\phi^{j_i}(\mathbf{x}_i)$ are normalized hydrogenlike orbitals for optimized effective charges. The continuum orbitals in Eq. (2) are also assumed to be hydrogenlike, but here we choose the single effective charge $Z_{\text{eff}} = 1.67$. We have found that in so doing a somewhat more realistic description of free electrons in the field of the He^{2+} nucleus was obtained than by using continuum orbitals that correspond to the optimized charges of the ground-state CI wave function.

Within the FCA the transition amplitude for DI at a given impact-parameter vector $\mathbf{b}$ takes the form

$$a_{i \to \mathbf{k}_1, \mathbf{k}_2}^{2e}(\mathbf{b}) = \frac{\varphi(k_{12})}{\sqrt{2}} \sum_{j_1 j_2} C_{j_1 j_2} [a_{j_1 \to \mathbf{k}_1}^{1e}(\mathbf{b}) a_{j_2 \to \mathbf{k}_2}^{1e}(\mathbf{b})$$

$$+ a_{j_1 \to \mathbf{k}_2}^{1e}(\mathbf{b}) a_{j_2 \to \mathbf{k}_1}^{1e}(\mathbf{b})], \qquad (3)$$

where $a_{j_i \to \mathbf{k}_i}^{1e}$ are single-ionization amplitudes obtained from effective one-electron calculations that do not account for dynamic correlation effects. In the present work the $a_{j_i \to \mathbf{k}_j}^{1e}$ were calculated in the *continuum distorted-wave with eikonal initial-state* (CDW-EIS) approximation [15,16] built upon the bound and continuum orbitals of Eqs. (2) and (3). We note that they were further multiplied by an appropriate overlap integral to correct for the nonorthogonality of bound and continuum orbitals constructed with respect to different effective charges.

Final-state correlations are incorporated in our model via the function $\varphi(k_{12})$ that appears in Eq. (2). We compare different explicit forms, all of which are based on the suggestion of Ref. [10] to approximate the widely used *3-Coulomb* (3C) wave function [18] by setting

$$\varphi(k_{12}) = e^{-\pi Z_{12}/(2k_{12})} \Gamma(1 - i Z_{12}/k_{12}) {}_1F_1(i Z_{12}/k_{12}; 1; -i k_{12} \alpha/2)$$

$$(4)$$

in Eq. (2). The parameter α in the argument of the confluent hypergeometric function ${}_1F_1$ can be interpreted as the average distance between both electrons. Its introduction removes spatial dependences in $\varphi(k_{12})$ and facilitates the calculations tremendously. The extreme choice $\alpha = 0$ yields ${}_1F_1 = 1$ such that the factor

$$|\varphi(k_{12})|^2 = \frac{Z_{12}}{k_{12}} \frac{2\pi}{e^{2\pi Z_{12}/k_{12}} - 1} \qquad (5)$$

appears in the transition probabilities and cross sections. This is the well-known *Coulomb density of states* (CDS) factor used in numerous previous investigations of DI by electron [19] and ion [20–23] impact. The CDS factor suppresses

exponentially the probability to find both emitted electrons with close momenta, but it ensures that electrons with very different final momenta move independently. Finite values for α in Eq. (4) relax the strong suppression at small momentum differences, but give the same limiting values for $k_{12} \to 0$ and $k_{12} \to \infty$ [24]. An obvious choice, which—among others—will be considered below is the average distance of the two electrons in the He ground state $\alpha \approx 1.4$ a.u. We will refer to the final-state model with finite α parameters as $3C^{av}$.

In the 3C model the interaction strength between the two continuum electrons is $Z_{12} = 1$. This choice yields too strong a repulsion between two low-energy electrons so that cross sections near threshold are typically much too small. This failure was corrected by introducing effective charges that depend on the momenta of both electrons [25]. Different explicit forms of such *dynamic screening* (DS3C) models have been proposed (see, e.g., Ref. [26], and references therein) and applied mainly to electron-induced single-ionization $(e, 2e)$ processes. Very recently, a somewhat simplified derivation of a DS3C model has been given and applied to $(e, 3e)$ reactions [27]. We exploit that work by using the proposed effective charge

$$Z_{12} = 1 - \frac{k_{12}}{(k_1 + k_2)^2} \qquad (6)$$

in Eq. (4) and refer to this model as $DS3C^{av}$.

Furthermore, we note that final-state correlations can be switched off by setting $\varphi(k_{12}) = 1$ in Eq. (3). The independent electron model (IEM) is recovered if in addition the He ground state is described by a single $1s^2$ configuration [i.e., by setting $j_1 = j_2 = 1s$ and $C_{1s^2} = 1$ in Eq. (1)]. For the sake of comparison we have performed such calculations. The corresponding results reported below rely on bound and continuum orbitals obtained from the exchange-only version of the optimized potential model (OPM) [28], which can be viewed as an appropriate definition of the no-correlation limit within density functional theory [29].

The correlation function under investigation was defined in Ref. [8] according to

$$R(k_{12}) = \frac{I_{cor}(k_{12})}{I_{unc}(k_{12})} - 1, \qquad (7)$$

where I_{cor} is the measured intensity for DI with a certain momentum difference k_{12}, while I_{unc} is the corresponding intensity for two electrons from independent events, i.e., from two data sets recorded at different times. A natural translation of this experimental ratio is a ratio of cross sections [10]

$$R(k_{12}) = \frac{\sigma^{tot} \int d\mathbf{k} \, d\Omega_{\mathbf{k}_{12}} \sigma(\mathbf{k}, \mathbf{k} + \mathbf{k}_{12})}{\int d\mathbf{k} \, d\Omega_{\mathbf{k}_{12}} \sigma(\mathbf{k}) \sigma(\mathbf{k} + \mathbf{k}_{12})} - 1, \qquad (8)$$

in which

$$\sigma(\mathbf{k}_1, \mathbf{k}_2) = \int d\mathbf{b} |a^{2e}_{i \to \mathbf{k}_1, \mathbf{k}_2}(\mathbf{b})|^2 \qquad (9)$$

is differential in the momenta of both emitted electrons,

$$\sigma(\mathbf{k}_1) = \int d\mathbf{k}_2 \sigma(\mathbf{k}_1, \mathbf{k}_2) \qquad (10)$$

is differential in the momentum of one electron, and

$$\sigma^{tot} = \int d\mathbf{k}_1 \sigma(\mathbf{k}_1) \qquad (11)$$

is the total DI cross section. Note that in both the numerator and denominator of Eq. (8) integrations over the solid angle between the electrons are performed such that R depends on the magnitude of the momentum difference $k_{12} = |\mathbf{k}_1 - \mathbf{k}_2|$ only.

III. RESULTS AND DISCUSSION

Let us now analyze the correlation function R by comparing the performance of different approximations to the initial and final two-electron states. We begin by showing in Fig. 1 CDW-EIS results obtained from the $3C^{av}$ final-state model with different α parameters and the CI initial-state wave function. The main characteristics of the experimental R for both 3.6 MeV/amu Au^{53+}-He and 100 MeV/amu C^{6+}-He collisions are positive maxima at around $k_{12} = 2$ a.u. and steep declines toward lower momentum differences. They are roughly reproduced by all $3C^{av}$ calculations. Only when the final-state repulsion is switched off does the shape of R change qualitatively. In this case, R increases and assumes positive values for $k_{12} \to 0$. One can thus conclude that the experimentally observed negative correlation at low momentum differences is caused by the final-state repulsion of the two electrons. This is, of course, no surprise and was discussed earlier in Refs. [8,10]: the primary effect of correlations in the final state is a strong suppression of two-electron emission with close momenta such that $I_{corr} \ll I_{unc}$ for small k_{12}.

Apart from these general features we observe that the positions and heights of the peaks as well as the behavior in the large k_{12} region are rather sensitive to α, and are different for both collision systems. Furthermore, despite the qualitative similarity with the experimental data none of our $3C^{av}$ calculations agrees particularly well with them. For $\alpha = 0$, i.e., the CDS model the disagreement is most pronounced: the peaks appear at too large k_{12}, and the curves decrease too rapidly toward $k_{12} \to 0$ in both cases. This implies that the final-state repulsion is too strong in this model. Increasing α, i.e., weakening the repulsion by assuming finite average distances between the electrons in their approximate relative wave function (4) improves the situation and shifts the peaks gradually toward smaller momentum differences. At the same time their heights increase, but only in the case of the 3.6 MeV/amu Au^{53+}-He system is this tendency significant. As a consequence, the correlation functions of both systems differ for finite α. Interestingly, the average distance of the electrons in the He ground state, $\alpha = 1.4$ a.u., is not the op-
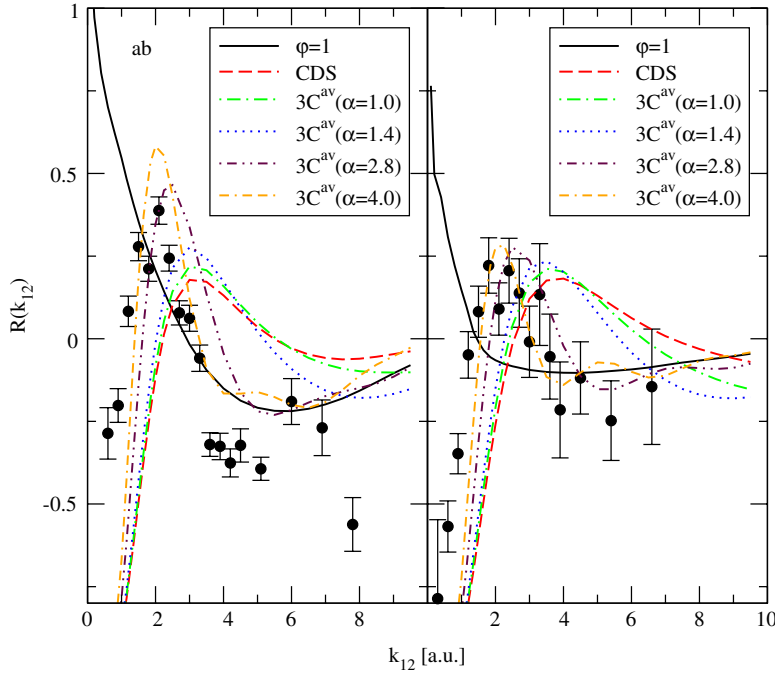
FIG. 1. (Color online) Correlation function R as a function of the momentum difference k_{12} of the ejected electrons for (a) 3.6 MeV/amu Au^{53+}-He and (b) 100 MeV/amu C^{6+}-He collisions calculated in the CDW-EIS approximation with CI initial-state wave function. Full lines ($\varphi=1$), no correlation in final states; dashed lines (CDS), $3C^{av}$ final-state model with $\alpha=0$; dot-dashed lines, $3C^{av}$ final-state model with $\alpha=1$ a.u.; dotted lines, $3C^{av}$ final-state model with $\alpha=1.4$ a.u.; dot-dot-dashed lines, $3C^{av}$ final-state model with $\alpha=2.8$ a.u.; dot-dash-dashed lines, $3C^{av}$ final-state model with $\alpha=4$ a.u.; (•), experimental results from [8].

timal choice, but only for a value as large as $\alpha=4$ a.u. are the experimental peak positions perfectly matched in both cases. The declines toward $k_{12} \rightarrow 0$ are still too rapid, and this deficiency persists for even larger α values, which we have not included in the figure for the sake of clarity.

A better account of the low k_{12} region is achieved in the DS3C^{av} model (Fig. 2), in which the strong repulsive character of the 3C wave function is alleviated. Let us exemplify this by considering back-to-back emission [i.e., $\cos(\mathbf{k}_1, \mathbf{k}_2)=-1$]. The effective charge (6) in the DS3C^{av} model is zero in this case, such that DI is not suppressed by final-state repulsion [$\varphi(k_{12})=1$ in Eq. (2)]. As a consequence,

there are non-negligible contributions to the numerator in the correlation function (8) even for low relative momenta. This is different in the 3C^{av} model, in which DI events at low k_{12} are erroneously suppressed for *all* relative electron angles. For example, the CDS factor is as small as 0.012 for $k_{12}=1$ a.u., such that the numerator in Eq. (8) is small and the correlation function is rather close to its minimum value $R=-1$ (cf. Fig. 1).

One can therefore conclude that the DS3C^{av} model is superior. However, Fig. 2 signals also some problems: First, higher values for α are needed to reproduce the experimental peak position, in particular, in the case of 3.6 MeV/amu
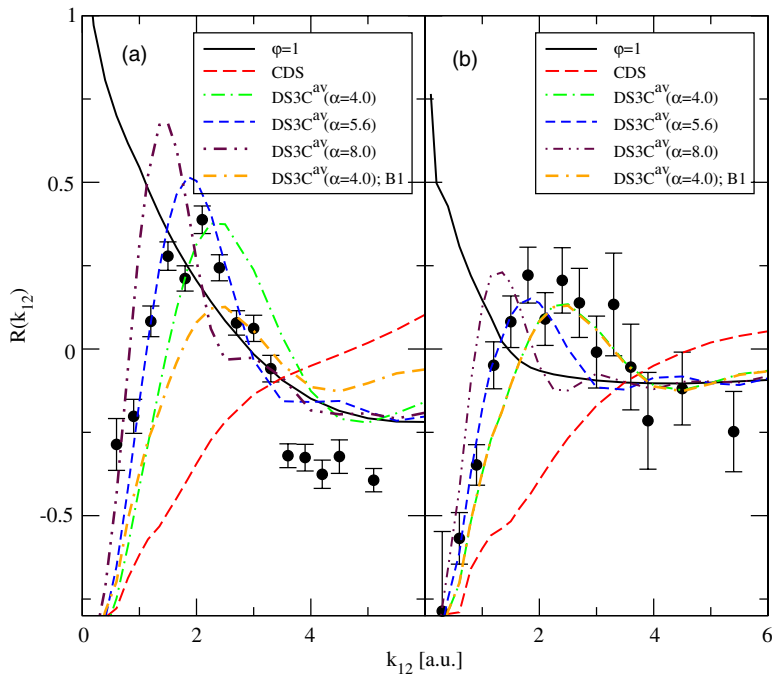
FIG. 2. (Color online) Correlation function R as a function of the momentum difference k_{12} of the ejected electrons for (a) 3.6 MeV/amu Au^{53+}-He and (b) 100 MeV/amu C^{6+}-He collisions calculated with CI initial-state wave function. Full lines ($\varphi=1$), CDW-EIS calculations without correlation in final states; long-dashed lines (CDS), CDW-EIS calculations with DS3C^{av} final-state model and $\alpha=0$, dot-dashed lines, CDW-EIS calculations with DS3C^{av} final-state model and $\alpha=4$ a.u.; short-dashed lines, CDW-EIS calculations with DS3C^{av} final-state model and $\alpha=5.6$ a.u.; dot-dot-dashed lines, CDW-EIS calculations with DS3C^{av} final-state model and $\alpha=8$ a.u.; dot-dash-dashed-lines, B1 calculations with DS3C^{av} final-state model and $\alpha=4$ a.u.; (•), experimental results from [8].
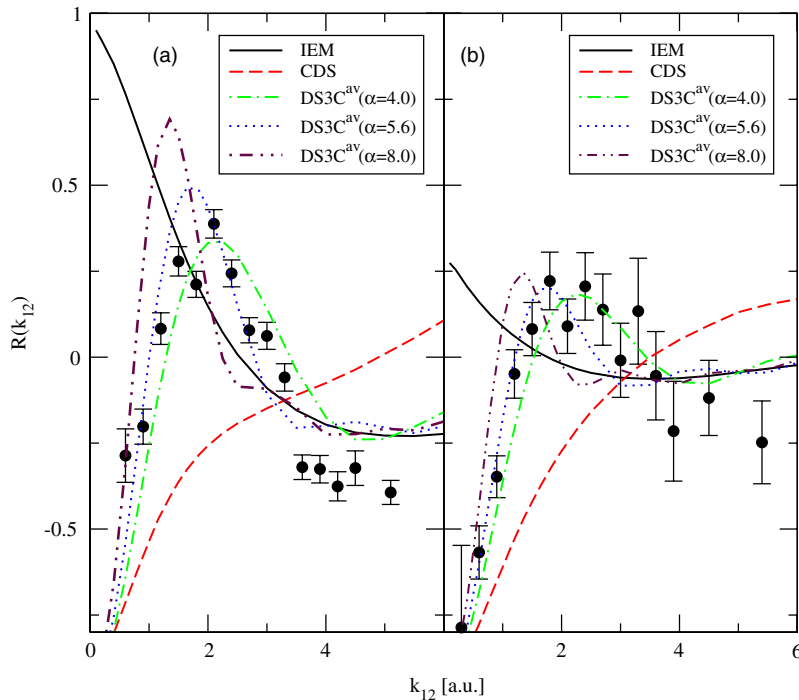
FIG. 3. (Color online) Correlation function R as a function of the momentum difference k_{12} of the ejected electrons for (a) 3.6 MeV/amu Au^{53+}-He and (b) 100 MeV/amu C^{6+}-He collisions calculated in the CDW-EIS approximation with (uncorrelated) OPM initial-state wave function. Full lines (IEM), no correlation in final states; dashed lines (CDS), DS3C^{av} final-state model and $\alpha=0$; dot-dashed lines, DS3C^{av} final-state model and $\alpha=4$ a.u.; dotted lines, DS3C^{av} final-state model and $\alpha=5.6$ a.u.; dot-dot-dashed lines, DS3C^{av} final-state model and $\alpha=8$ a.u.; (•), experimental results from [8].

Au^{53+}-He collisions. The CDS results ($\alpha=0$) exhibit no peak at all in the momentum range shown and appear much more unrealistic than their 3C^{av} counterparts. Second, the DS3C^{av} calculations turned out to be rather sensitive to numerical inaccuracies in the transition amplitudes. This is due to the oscillating character of the confluent hypergeometric function in Eq. (4) in conjunction with the momentum dependence of Z_{12} [Eq. (6)]. At large relative momenta, where DI is unlikely and the amplitudes are very small we have not succeeded in obtaining reliable results. Therefore, we restrict the presentation of R to the $k_{12} \leq 6$ a.u. region in Fig. 2. Third, we have found that other variants of DS3C^{av} models, e.g., relying on the effective charge Z_{12} of Ref. [26] yield results, which are somewhat different from those shown in Fig. 2. At first sight this was surprising since the models seem to be rather similar. A closer inspection of our numerical results showed, however, that small differences in the doubly differential cross sections (9) can accumulate to rather significant values in the process of the numerous integrations involved in the calculation of R.

In addition to using the CDW-EIS method we have performed some test calculations in the first Born (B1) approximation. They are included in Fig. 2 for the parameter $\alpha=4$ a.u., which gives the best description of R in the case of the 100 MeV/amu C^{6+}-He collision system. At high impact velocity v_P the B1 correlation function is independent of the perturbation strength defined as the ratio of projectile charge Z_P and v_P due to the scaling properties of the B1 transition amplitudes [4]. Hence, we have obtained the same results for both collision systems. In the case of 100 MeV/amu C^{6+}-He collisions, for which the perturbation is small ($Z_P/v_P \approx 0.1$) we observe that the B1 result practically coincides with that obtained from the CDW-EIS approximation. This is different for the 3.6 MeV/amu Au^{53+}-He system ($Z_P/v_P \approx 4.4$). In this case, the B1 correla-

tion function has the same shape and peak position as its CDW-EIS counterpart, but the peak height is considerably reduced and clearly below the experimental value. This suggests that the maximum of R increases with increasing interaction strength, i.e., its dependence on the collision dynamics cannot be ignored completely, although it is certainly weaker than that of the DI cross section itself. We note that the experimental data support this trend, but the error bars are too large to state this with certainty.

From Figs. 1 and 2 one is tempted to conclude that only final-state correlations are visible in the correlation function, and an accurate final-state model might yield perfect agreement with the experimental data. Apparently, our "α-models" are too crude to achieve this goal, but they show that refinements should be built upon the idea of dynamically screened effective charges. It would be interesting to see whether a full DS3C calculation would give completely satisfactory agreement with the experimental R. This cannot be taken for granted since some problems have been observed in this model for fully differential $(e,3e)$ cross sections when electron energies were of the order of or greater than their initial binding energies [27]. In any case, a full DS3C calculation would be much more demanding than the present one, since the two-electron transition amplitude would no longer be given as a sum of products of single-electron amplitudes [cf. Eq. (3)].

The dominance of the final-state repulsion raises also the question whether initial-state correlations play *any* role in determining the shape of R. In order to shed light on this issue results obtained with an uncorrelated $1s^2$ initial state within the OPM central-field model are shown in Fig. 3. In fact, one can hardly observe any difference to the results of Fig. 2, for which the CI wave function of Ref. [17] was used. Remarkably, this remains true when the final-state repulsion is also switched off. We thus observe that a completely

uncorrelated IEM calculation yields a nonzero correlation function—a behavior that contradicts the very idea of its definition. This happens because R is defined on the level of cross sections in Eq. (8) instead of impact-parameter dependent transition probabilities. With the definitions

$$p_s(\mathbf{k},\mathbf{b}) = |a_{1s \to \mathbf{k}}^{1e}(\mathbf{b})|^2 \qquad (12)$$

and

$$P_s(\mathbf{b}) = \int d\mathbf{k}\, p_s(\mathbf{k},\mathbf{b}) \qquad (13)$$

the correlation function (8) for uncorrelated states can be cast into the form

$$R^{\mathrm{IEM}}(k_{12}) = \frac{\sigma^{\mathrm{tot}} \int d\mathbf{k}\, d\Omega_{\mathbf{k}_{12}} \int d\mathbf{b}\, p_s(\mathbf{k},\mathbf{b}) p_s(\mathbf{k}+\mathbf{k}_{12},\mathbf{b})}{\int d\mathbf{k}\, d\Omega_{\mathbf{k}_{12}} \int d\mathbf{b}\, P_s(\mathbf{b}) p_s(\mathbf{k},\mathbf{b}) \int d\mathbf{b}'\, P_s(\mathbf{b}') p_s(\mathbf{k}+\mathbf{k}_{12},\mathbf{b}')} - 1, \qquad (14)$$

where the total DI cross section is given by

$$\sigma^{\mathrm{tot}} = \int d\mathbf{b}\, P_s^2(\mathbf{b}). \qquad (15)$$

The symmetrization of the final state (2) can be ignored in the IEM. Obviously, the different integrations over the impact-parameter vector $\mathbf{b}$ in the numerator and denominator prevent R from collapsing to the expected trivial result $R^{\mathrm{IEM}}(k_{12})=0$. We note that the integration over $\mathbf{b}$ is also implicit in the experimental correlation function, since events for all momentum transfers have been collected in the yields I_{cor} and I_{unc}.

According to Fig. 3 R^{IEM} exhibits the following general characteristics: at intermediate and larger momentum differences its dependence on k_{12} is rather weak and its value close to zero, while it increases and assumes positive values for $k_{12} \to 0$. We have spent some efforts to analyze and interpret this behavior, but found that one can provide at best qualitative arguments because of the many integrations involved.

Low k_{12} values correspond to situations where the momenta of both electrons are similar. This region is dominated by soft electrons, whose single-ionization probabilities $p_s(\mathbf{k},\mathbf{b})$ are broadly distributed over the impact parameter. In I_{cor} one integrates the product of two very similar single-particle transition probabilities over $\mathbf{b}$, while in I_{unc} two independent integrals over products of $\mathbf{k}$-dependent and $\mathbf{k}$-integrated probabilities are calculated and multiplied afterwards. We have checked for a few specific examples with fixed momenta and ejection angles that the integrated product is indeed in almost all cases larger than the product of integrals, such that even after the multiplication with the total DI cross section (which is smaller than one in atomic units) does the numerator remain larger than the denominator, i.e., $I_{\mathrm{cor}} > I_{\mathrm{unc}}$.

At large k_{12} electron pairs, in which one has a small momentum and the other a large one contribute strongly to I_{cor} and I_{unc}. Fast electrons occur dominantly at small impact parameters. If one assumes that in some limit the corre-

sponding single-ionization probabilities are constant for $0<b<b_{\mathrm{max}}$, zero for $b>b_{\mathrm{max}}$, and furthermore independent of the (large) momentum one can show that $I_{\mathrm{cor}}=I_{\mathrm{unc}}$. The details of our numerical calculations show, however, that this limit—if existing—is not yet reached at the largest k_{12} that we could consider. For instance, we found that also electron pairs with two fast partners play a non-negligible role in this region, and the single-ionization probabilities tend to decrease with increasing momentum instead of being constant. Thus, we cannot even say with certainty that the limit $R^{\mathrm{IEM}}=0$ is reached for DI at large momentum differences.

Returning to the question whether the initial state influences the correlation function let us compare the CI and OPM results obtained with uncorrelated final states. The corresponding full curves in Figs. 2 and 3 are almost indistinguishable in the case of the 3.6 MeV/amu Au^{53+}-He collision system, while slight deviations can be observed for 100 MeV/amu C^{6+}-He collisions. In the language of many-body perturbation theory [1,30] this can be interpreted in the following way: in the strongly perturbing 3.6 MeV/amu Au^{53+}-He case DI occurs predominantly by two independent projectile-electron interactions, i.e., by a second-order ('TS1') process, which is not very sensitive to electronic correlations. In the case of the weakly perturbing carbon projectiles the first-order transition amplitude, which is nonzero only if initial and/or final states are correlated gains importance. Hence, the similarities in R in the former, and the slight differences in the latter case when calculated with or without correlated initial-state wave functions might reflect the role of the first-order amplitude. We note that one can view this amplitude as an analog to the widely discussed shake-off process, which is understood as one direct projectile-electron interaction leading to single ionization followed by the "shake-off" of the second electron as a consequence of the unscreening of the nucleus [1].

Some further remarks are in order at this point. First, the given explanation is at best of a qualitative nature, since our frozen-correlation CDW-EIS approach cannot be linked directly to specific amplitudes of many-body perturbation
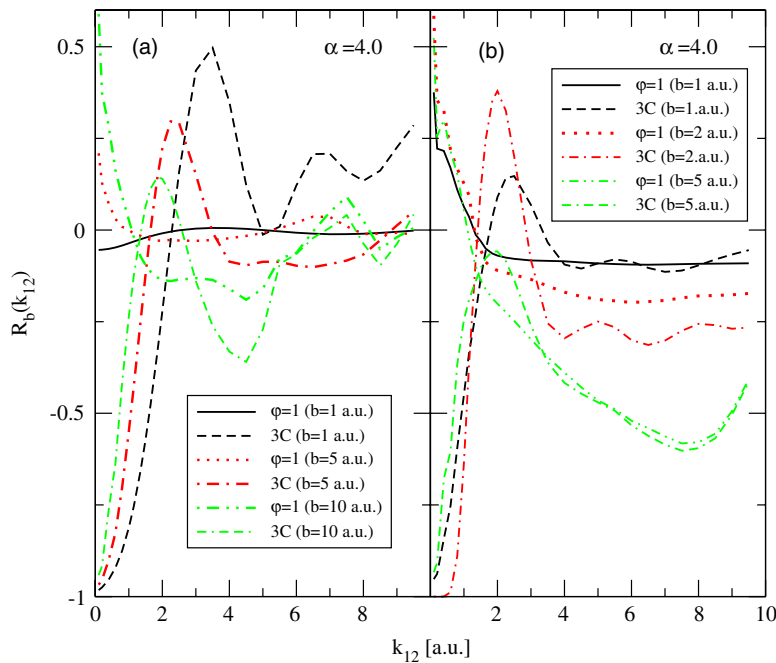
FIG. 4. (Color online) Correlation functions R_b for fixed impact parameters b as functions of the momentum difference k_{12} of the ejected electrons for (a) 3.6 MeV/amu Au^{53+}-He and (b) 100 MeV/amu C^{6+}-He collisions calculated in the CDW-EIS approximation with CI initial-state wave functions. The lines referred to as $\varphi=1$ correspond to calculations without correlation in the final states, those referred to as 3C correspond to the $3C^{av}$ final-state model with $\alpha=4$ a.u.

theory. Second, from Figs. 2 and 3 it is apparent that the traces of initial-state correlations are covered by the final-state repulsion as soon as the latter is switched on. One promising way to circumvent this dominance of the final state is to restrict the events collected in R to back-to-back electron emission, which should not be affected by electron-electron repulsion [12]. Third, we note that the above-metioned R calculations of Ref. [10] were based on a direct modeling of the shake-off mechanism, which is a correlated electron-emission process, in conjunction with the 3C^{av} final-state model. It was found that the competition of interferences between direct and exchange amplitudes and the final-state repulsion were crucial for forming the characteristic shape of R. The dependence of the results on the α values used was much weaker than in our study, which can probably be attributed to the simplifying assumptions used in Ref. [10]. From the qualitative agreement with the experimental data for 100 MeV/amu C^{6+}-He collisions it was concluded that DI processes other than shake-off were unimportant.

Our refined higher-order calculations give a somewhat different picture. Namely, the characteristic shape of R is obtained without resorting to the shake-off or any other specific DI mechanism and interferences between corresponding amplitudes. According to our analysis the shape originates from the interplay between the final-state repulsion and a rather general behavior of ionization probabilities when integrated over the impact parameter. The latter effect has nothing to do with electronic correlations, which is why we think that the definition of the correlation function on the level of cross sections is not completely satisfactory.

It is thus of interest to avoid the integration over the impact parameter and to study the correlation function for fixed (scalar) b values. Corresponding results are shown in Fig. 4. Reinspecting Eq. (14) we first note that in this case $R_b^{IEM}=0$ for all k_{12} such that any structure in the curves is indeed related to electronic correlations. In order to elucidate their

role we have included two sets of calculations in Fig. 4 for three different impact parameters: in the first set only initial-state correlations are included via the CI wave function of Ref. [17], while in the second one also final-state correlations are considered in terms of the 3C^{av} model with $\alpha=4$ a.u. We note that the DS3C^{av} final-state model yields comparable results.

We observe that the shapes of $R_b(k_{12})$ exhibit the same general trends as the b-integrated correlation functions when correlations are included in both the initial and final states: a maximum at intermediate k_{12} and a steep decline for $k_{12} \to 0$. However, the details are different and depend strongly on b. With increasing b the positions of the maxima shift toward smaller momentum differences and the peak heights decrease. For the 100 MeV/amu C^{6+}-He system they become even negative. On the right sides of the main maxima further structures appear, particularly for the 3.6 MeV/amu Au^{53+}-He system. We note that qualitatively similar results are obtained when initial-state correlations are neglected. This implies that the b-dependent correlation function mirrors the properties of the final-state model used rather directly.

The structures change, but do not vanish when the final-state correlations are switched off, i.e., also initial-state correlations do play a role. The low k_{12} region is most significantly altered by the omission of electron-electron repulsion in the final state: with the exception of the result for 3.6 MeV/amu Au^{53+}-He at $b=1$ a.u. the curves increase and assume positive values for $k_{12} \to 0$. Overall and in line with the interpretation from the viewpoint of many-body perturbation theory given above one observes the tendency that the effects of initial-state correlations on R increase with decreasing perturbation strength: they gain importance with increasing impact parameters, and—as already observed for the **b**-integrated case (cf. Figs. 2 and 3)—they are more pronounced for 100 MeV/amu C^{6+}-He than for 3.6 MeV/amu Au^{53+}-He collisions. Thus, the b-differential level would of-

fer the chance to study seperate collision mechanisms and the associated initial-state correlations in closer detail, if they were not overwhelmed by the effects of the final-state repulsion.

Of course, the b-differential level cannot be realized in an experiment directly, but it is well known that at projectile scattering angles θ larger than $1/(\mu v_P)$ (where μ denotes the reduced mass of the heavy-particle motion) one can assume a classical relation between b and θ [31]. Together with the above-mentioned disappearance of final-state repulsion for back-to-back emission one can infer that a scattering-angle specific sampling of back-to-back DI events would allow a direct and unambiguous view on the workings of initial-state correlations.

IV. CONCLUDING REMARKS

In this work we have investigated the correlation function R for double ionization from the viewpoint of the frozen-correlation approximation. Dynamic correlation effects are neglected in this framework, but initial- and final-state correlations were taken into account on the basis of different models. The single-particle ionization amplitudes were calculated in the continuum distorted-wave with eikonal initial-state approximation, which allows not only consideration of weak, but also rather strong perturbations.

The comparisons of the calculated correlation functions with experimental data for 3.6 MeV/amu Au^{53+}-He and 100 MeV/amu C^{6+}-He collisions support earlier conclusions about the dominance of the final-state repulsion in shaping R as a function of the momentum difference of both emitted electrons. However, our study shows that the popular Coulomb density of states factor and also a simplified 3C final-state wave function are too crude to explain the data quantitatively. The introduction of dynamic screening improves the situation, but quantitative agreement with the measurements has not been achieved, yet. This might be due to our simplified final-state model that allows the calculation of the two-electron ionization amplitude from an appropriate combination of one-electron amplitudes, but it is not clear whether a full DS3C calculation would resolve the discrepancies.

We have pointed out that the interpretation of R is biased by the fact that integrations over the impact parameter (or, alternatively, the momentum transfer) are implicit in its definition. As a consequence of this integration, even an independent electron calculation gives a nontrivial result with generally increasing values for R toward zero momentum difference. Our calculations suggest that the interplay of this tendency and the final-state repulsion is largely responsible for the characteristic shape of R, while initial-state correlations play at most a marginal role.

Only on the impact-parameter-differential level is the correlation function an unambiguous probe of electron-correlation effects, since here an independent electron calculation must give $R=0$. Similar to the integrated case, the final-state repulsion dominates possible effects of the initial state, and the details are rather sensitive to the final-state model used. Initial-state effects should become more apparent if one would restrict the events collected in R to back-to-back double ionization, where the target nucleus shields the electron-electron repulsion. Earlier work demonstrated that the statistics of the experimental data were sufficient to impose this restriction on the integrated level [12]. Keeping in mind that for not too low momentum transfer the impact parameter can be related classically to the measurable scattering angle even the b-differential level can, in principle, be considered, although very small counting rates would make the analysis tedious and challenging. We believe that such an attempt would be worthwhile, since it is only on this level that structures in R can be related to electron-correlation effects unambiguously. Back-to-back impact-parameter-differential data probably provide a very sensitive probe for initial-state correlations.

Finally, let us mention that despite the usefulness of the correlation function it appears also important to continue with tracing effects of initial- and final-state correlations directly in multi- and possibly fully differential electron-emission patterns. We have embarked on this task in the framework of the two-electron models presented here and will report results in a forthcoming paper.

[1] J. H. McGuire, *Electron Correlation Dynamics in Atomic Collisions* (Cambridge University Press, Cambridge, England, 1997).

[2] *Many-Particle Quantum Dynamics in Atomic and Molecular Fragmentation*, edited by J. Ullrich and V. P. Shevelko (Springer, Heidelberg, 2003).

[3] J. Berakdar, A. Lahham-Bennani, and C. D. Cappello, Phys. Rep. **374**, 91 (2003).

[4] N. Stolterfoht, R. D. DuBois, and R. D. Rivarola, *Electron Emission in Heavy Ion-Atom Collisions* (Springer, Berlin, 1997).

[5] R. Dörner, V. Mergel, O. Jagutzki, L. Spielberger, J. Ullrich, R. Moshammer, and H. Schmidt-Böcking, Phys. Rep. **330**, 95 (2000).

[6] J. Ullrich, R. Moshammer, A. Dorn, R. Dörner, L. P. H. Schmidt, and H. Schmidt-Böcking, Rep. Prog. Phys. **66**, 1463 (2003).

[7] D. Fischer, R. Moshammer, A. Dorn, J. R. Crespo Lopez-Urrutia, B. Feuerstein, C. Höehr, C. D. Schröeter, S. Hagmann, H. Kollmus, R. Mann, B. Bapat, and J. Ullrich, Phys. Rev. Lett. **90**, 243201 (2003).

[8] M. Schulz R. Moshammer, W. Schmitt, H. Kollmus, B. Feuerstein, R. Mann, S. Hagmann, and J. Ullrich, Phys. Rev. Lett. **84**, 863 (2000).

[9] B. Feuerstein, M. Schulz, R. Moshammer, and J. Ullrich, Phys. Scr., T **T92**, 447 (2001).

[10] L. G. Gerchikov and S. A. Sheinermann, J. Phys. B **34**, 647 (2001).

[11] L. G. Gerchikov, S. A. Sheinermann, M. Schulz, R. Moshammer, and J. Ullrich, J. Phys. B **35**, 2783 (2002).

[12] M. Schulz, R. Moshammer, L. G. Gerchikov, S. A. Sheinermann, and J. Ullrich, J. Phys. B **34**, L795 (2001).

[13] M. Schulz, D. Fischer, R. Moshammer, and J. Ullrich, J. Phys. B **38**, 1363 (2005).

[14] F. Martín and A. Salin, Phys. Rev. A **54**, 3990 (1996).

[15] D. S. F. Crothers and J. F. McCann, J. Phys. B **16**, 3229 (1983).

[16] P. D. Fainstein, L. Gulyás, and A. Salin, J. Phys. B **29**, 1225 (1996).

[17] J. N. Silverman, O. Platas, and F. A. Matsen, J. Chem. Phys. **32**, 1402 (1960).

[18] M. Brauner, J. S. Briggs, and H. Klar, J. Phys. B **22**, 2265 (1989).

[19] C. D. Cappello, B. Joulakian, and J. Langlois, J. Phys. IV **3**, 125 (1993).

[20] M. McCartney, J. Phys. B **30**, L155 (1997).

[21] S. Keller, B. Bapat, R. Moshammer, J. Ullrich, and R. M. Dreizler, J. Phys. B **33**, 1447 (2000).

[22] J. Bradley, R. J. S. Lee, M. McCartney, and D. S. F. Crothers, J. Phys. B **37**, 3723 (2004).

[23] M. Fiori, A. B. Rocha, C. E. Bielschowsky, G. Jalbert, and C. R. Garibotti, J. Phys. B **39**, 1751 (2006).

[24] T. Kirchner, L. Gulyás, R. Moshammer, M. Schulz, and J. Ullrich, Nucl. Instrum. Methods Phys. Res. B **205**, 479 (2003).

[25] J. Berakdar and J. S. Briggs, Phys. Rev. Lett. **72**, 3799 (1994).

[26] S. Zhang, J. Phys. B **33**, 3545 (2000).

[27] J. R. Götz, M. Walter, and J. S. Briggs, J. Phys. B **38**, 1569 (2005).

[28] E. Engel and S. H. Vosko, Phys. Rev. A **47**, 2800 (1993).

[29] E. Engel and R. M. Dreizler, J. Comput. Chem. **20**, 31 (1999).

[30] L. Nagy, J. H. McGuire, L. Végh, B. Sulik, and N. Stolterfoht, J. Phys. B **30**, 1939 (1997).

[31] P. T. Greenland, J. Phys. B **14**, 3707 (1981).